CHEMISTRY
A EUROPEAN JOURNAL

DOI: 10.1002/chem.200601736

The Mechanism of C−X (X = F, Cl, Br, and I) Bond Activation in CX_4 by a Stabilized Dialkylsilylene

Chi-Hui Chen and Ming-Der Su*[a]

Abstract: The potential-energy surfaces for the abstraction and insertion reactions of dialkylsilylene with carbon tetrahalides (CX_4) have been characterized in detail using density functional theory (B3LYP), including zero-point corrections. Four CX_4 species, CF_4, CCl_4, CBr_4, and CI_4, were chosen as model reactants. The theoretical investigations described herein suggest that of the three possible reaction paths, the one-halogen-atom abstraction (X abstraction), the one-CX_3-group abstraction (CX_3 abstraction), and the insertion reaction, the X-abstraction reaction is the most favorable, with a very low activation energy. However, the insertion reaction can lead to the thermodynamically stable products. Moreover, for a given stable dialkylsilylene, the chemical reactivity has been found to increase in the order $CF_4 \ll CCl_4 < CBr_4 < CI_4$, that is, the heavier the halogen atom (X), the more facile is its reaction with a stable dialkylsilylene. In particular, halogen abstraction is always predicted to be much more favorable than abstraction of a CX_3 group from both energetic and kinetic viewpoints. In brief, electronic as well as steric factors play a crucial role in determining the chemical reactivity of the haloalkane species, kinetically as well as thermodynamically. Our conclusions based on the results of our theoretical investigations are in accordance with available experimental observations. Furthermore, a configuration-mixing model based on the work of Pross and Shaik has been used to rationalize the computational results. The results obtained allow a number of predictions to be made.

Keywords: density functional calculations · kinetics · reaction mechanisms · silicon · thermodynamics

Introduction

Stable silylenes based on imidazole heterocycles (**1**–**4**) have attracted widespread interest owing to their inherent stability[1] and their interesting structural and bonding features.[2] As a result, the availability of stable silylenes has allowed the discovery of new compounds and novel reaction chemistry.[3] These successful synthetic results have demonstrated that such a heterocyclic framework can lend considerable stability to a silicon-containing ring through aromatic π-electron delocalization. After the discovery of *N*-heterocyclic stable crystalline silylenes **1**–**4**,[4–7] Kira et al. reported the synthesis of the first isolable dialkylsilylene **5**[8] with no such nitrogen stabilization. That is, this species is distinct from silylenes **1**–**4** in that its stability is derived entirely from steric protection of the divalent silicon atom by the two $SiMe_3$ groups attached to each of the two α-carbon atoms. It is thus commonly recognized that dialkylsilylene **5** should be a stable silylene and its reactivity towards a range of organic, inorganic, and organometallic substrates should also continue to be explored.

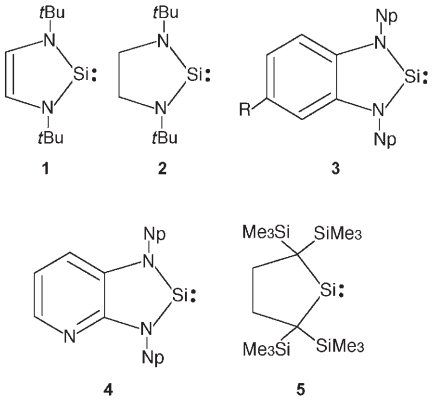

In fact this situation has changed greatly during the past five years and our knowledge of the chemical properties of dialkylsilylene **5** has significantly improved. In particular, the reactions of **5** with halogenated hydrocarbons yielded

[a] C.-H. Chen, Prof. Dr. M.-D. Su
Department of Applied Chemistry, National Chiayi University
Chiayi 60004 (Taiwan)
Fax: (+886) 05-2717901
E-mail: midesu@mail.ncyu.edu.tw

products remarkably different to those obtained using other stable silylenes (such as **1** and **2**).[1c] For instance, as shown in Scheme 1, with the haloalkane $CXCl_3$ (X = Cl or H), dichlorosilane **6** was isolated in high yield, whereas addition

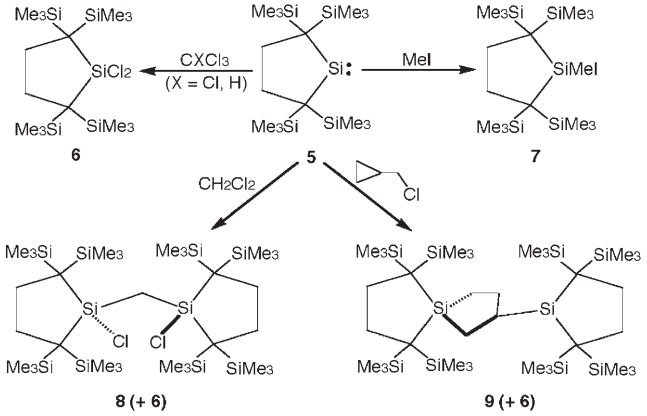

Scheme 1. Reactions of dialkylsilylene **5** with halogenated hydrocarbons.

of CH_3I exclusively gave the corresponding iodo(methyl)silane **7**. In contrast, reaction of **5** with CH_2Cl_2 gave the double insertion product **8** and a small amount of **6**. On the other hand, reaction of **5** with (chloromethyl)cyclopropane produced the unusual spiro[4,4]nonane derivative **9** and **6**. As observed in similar reactions of **1** and **2**, the above reactions proceed selectively to produce radical-coupling products such as Cl_3CCCl_3 and HCl_2CCCl_2H, which were found in the reaction of **5** with CCl_4 and $CHCl_3$. From these findings, West and Hill suggested that these reactions can be explained in terms of a radical pathway (or a single-electron-transfer mechanism).[1c] Namely, for example, homolytic scission of the C–Cl bond gives the carbon radical and the chlorinated silyl radical. Then, recombination of the silyl radical and another chlorine radical, formed by chlorine abstraction from another haloalkane, can give the observed coupling product, dichlorosilane **6**.

This motivated us to investigate the mechanisms for the chemical reaction of dialkylsilylene with haloalkanes. Basically, as in organometallic systems,[9] two kinds of reaction pathway can be involved. One is a radical mechanism proceeding by single-electron transfer (SET) and either halogen-atom (X) or CX_3-group abstraction [see Eq. (1); {silylene} represents the stable dialkylsilylene **10**].[10] The other is an insertion mechanism in which the central silicon atom of the dialkylsilylene inserts into the C–X bond of the haloalkane [Eq. (2)].

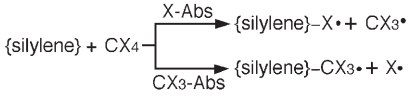

(1)

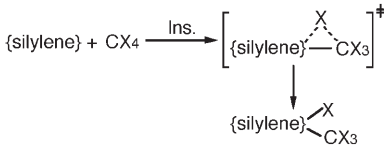

(2)

In fact, to the best of our knowledge, until now neither experimental nor theoretical resources have been devoted to the study of the mechanism of the reaction of a dialkylsilylene with haloalkanes. As a result of the experimental difficulties in handling such reactions, their reaction barriers and their spectroscopic features are still not well understood. It is astonishing how little is known about the mechanisms of this reaction considering the importance of silylene in organic synthesis and coordination chemistry and the extensive research activity on other bottle-stable silylene species (such as **1** and **2**).[1–3]

To study this reaction, it is necessary to determine the optimum intermediate and transition-state geometries of the molecules as well as the ground-state energies of the decomposition products. Consequently, we undertook to investigate the potential-energy surfaces of the model reactions in Equation (3) by using density functional theory (DFT). That is, we have explored theoretically three kinds of reaction paths for the model reaction between CX_4, where X = F, Cl, Br, and I, and a coordinatively unsaturated dialkylsilylene. These three reaction pathways are 1) the one-halogen-atom abstraction reaction, which is named **X-Abs** [Eq. (3a)], 2) the one-CX_3-group abstraction reaction, which is named **CX_3-Abs** [Eq. (3b)], and 3) the C–X bond insertion reaction, which is named **InS** [Eq. (3c)]. For simplicity, the specific dialkylsilylene system we have investigated is 2,2,5,5-tetrakis(silyl)silacyclopentane-1,1-diyl (**10**).[10]

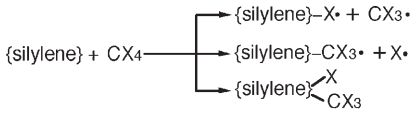

(3a)
(3b)
(3c)

The purpose of this work was fourfold: 1) To determine which reaction pathway predominates and to provide essential information about the mechanism of the reaction, 2) to obtain a detailed understanding of the energetics and kinetics of the transfer of either a halogen atom or a CX_3 group from CX_4 to dialkylsilylene, 3) to probe the dominant factors affecting the reactivities of a variety of halocarbons, and 4) to obtain a better understanding of the origin of barrier heights for such dialkylsilylene reactions. From these investigations, a better understanding of the thermodynamic and kinetic aspects of such dialkylsilylene reactions with haloalkanes may shed some light on the optimal design of further related synthetic and catalytic processes.

Computational Methods

All geometries were fully optimized without imposing any symmetry constraints, although in some instances the resulting structure showed various elements of symmetry. The geometries and energetics of the stationary points on the potential-energy surface were calculated by using the DFT (B3LYP)[11] method in conjunction with the 6-311G(d) basis set.[12] We denote our B3LYP calculations by B3LYP/6-311G(d). The spin-unrestricted (UB3LYP) formalism used for the open-shell (doublet) species and their $<S^2>$ expectation values were nearly all equal to the ideal value (0.75). Therefore their geometries and energetics are reliable for this study. Vibrational frequency calculations at the B3LYP/6-311G(d) level of theory were used to characterize all stationary points as either minima (the number of imaginary frequencies (NIMAG) = 0) or transition states (NIMAG = 1). The relative energies are thus corrected for vibrational zero-point energies (ZPE, not scaled). Thus, only the singlet potential-energy surface was considered throughout this work. All of the DFT calculations were performed using the Gaussian 03 package of programs.[13]

Results and Discussion

Geometries and energetics of dialkylsilylene: The predicted geometrical parameters for the closed-shell dialkylsilylene species, based on the B3LYP/6-311G(d) level of theory, are collected in Scheme 2 and are compared with some available

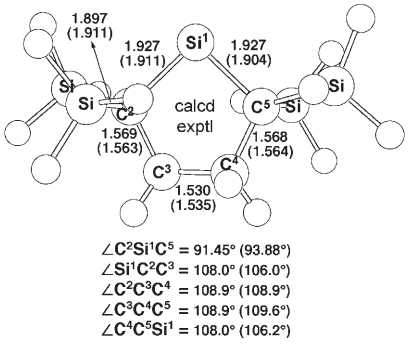

Scheme 2. Predicted geometrical parameters for the closed-shell dialkylsilylene species based on B3LYP/6-311G(d) calculations along with some available experimental values.

experimental values.[8] As mentioned earlier, we have used SiH_3 substituent groups, instead of $SiMe_3$ groups,[10] in the stable dialkylsilylene molecule (**10**) for the sake of simplicity. Nevertheless, as seen in Scheme 2, the molecular parameters for our B3LYP calculations agree reasonably well with the available experimental data. For instance, the calculated Si–C and C–C bond lengths in the five-membered ring shown in Scheme 2 are in good accord with experimental data.[8] The bond lengths and angles are in agreement to within 0.02 Å and 2.0°, respectively. In particular, it is interesting that the B3LYP value for the ∢C2C3C4 bond angle (108.9°) in **10** is in perfect agreement with the experimental data.[8] However, the calculated ∢C2SiC5 angle in **10** is predicted to be smaller by about 2.4° than the corresponding experimental value.[8] In any event, the good agreement between our computational results and the available experimental results is quite encouraging. We are therefore confident that the B3LYP/6-311G(d) calculations can provide an adequate theoretical level for further investigations of the molecular geometries and energetic features of the reaction of dialkylsilylene with haloalkanes.

The fully optimized geometries calculated at the B3LYP/6-311G(d) level of theory for the reactants, precursor complexes (**Pcx**), transition states (**TS**), and products (**Pro**) of the three kinds of reaction mechanisms described earlier are shown in Figures 1, 2, 3, and 4 for CF_4, CCl_4, CBr_4, and CI_4,

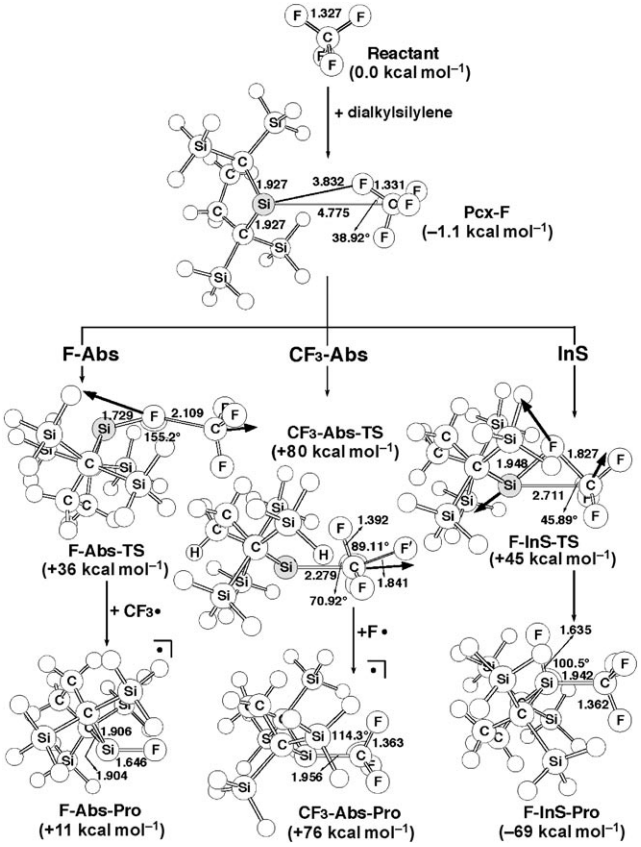

Figure 1. The optimized geometries (in Å and °) for the reactants, precursor complexes (**Pcx**), transition states (**TS**), and products (**Pro**) in the reaction of a stable dialkylsilylene with CF_4 through three reaction pathways, that is, the one-fluorine-atom abstraction (**F-Abs**), the one-CF_3-group-abstraction (**CF_3-Abs**), and the insertion reaction (**F-InS**). All were calculated at the B3LYP/6-311G(d) level of theory. The heavy arrows indicate the main components of the transition vector. Hydrogen atoms have been omitted for clarity.

respectively. For convenience, we have also given the energies relative to the two reactant molecules, that is, dialkylsilylene (**10**) + CX_4 (X = F, Cl, Br, and I). The relative energies for the various reaction mechanisms are summarized in Table 1. To simplify the comparisons and to emphasize the trends, the calculated heats of reaction and the individual barrier heights are also listed in Table 1.

Mechanism for the radical reactions: We first consider the radical mechanisms that proceed by single-electron transfer

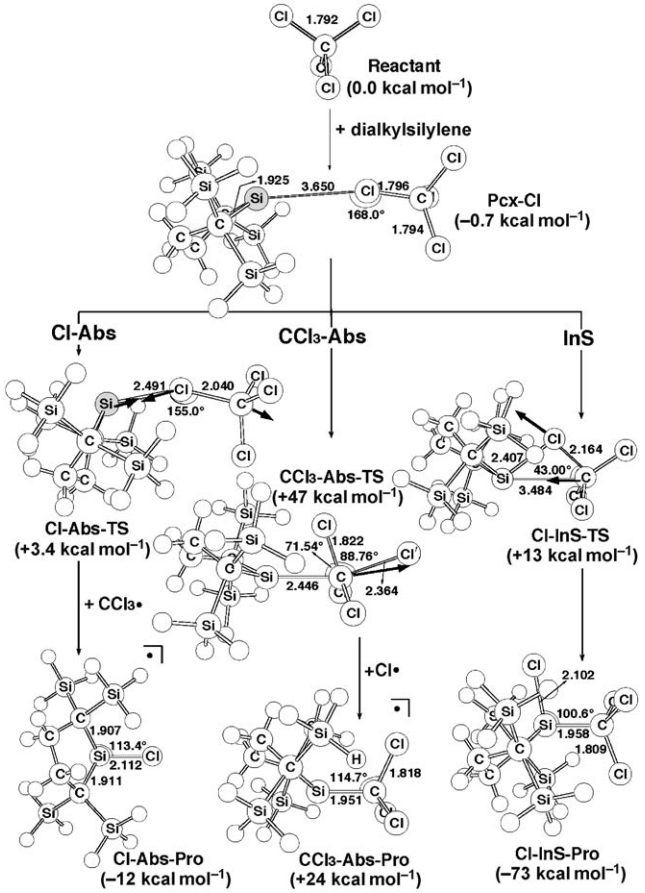

Figure 2. The optimized geometries (in Å and °) for the reactants, precursor complexes (**Pcx**), transition states (**TS**), and products (**Pro**) in the reaction of a stable dialkylsilylene with CCl_4 through three reaction pathways, that is, the one-chlorine-atom abstraction (**Cl-Abs**), the one-CCl_3-group-abstraction (**CCl_3-Abs**), and the insertion reaction (**Cl-InS**). All were calculated at the B3LYP/6-311G(d) level of theory. The heavy arrows indicate the main components of the transition vector. Hydrogen atoms have been omitted for clarity.

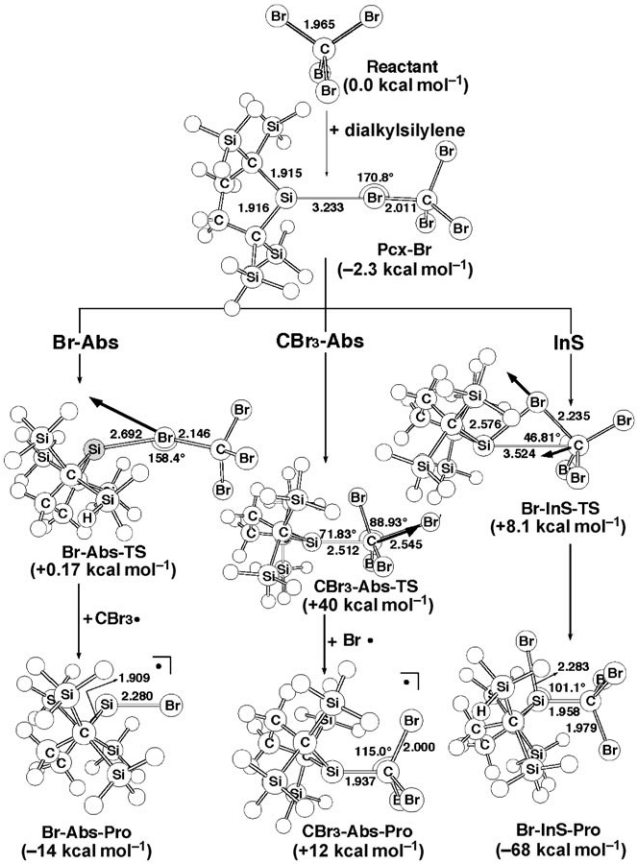

Figure 3. The optimized geometries (in Å and °) for the reactants, precursor complexes (**Pcx**), transition states (**TS**), and products (**Pro**) in the reaction of a stable dialkylsilylene with CBr_4 through three reaction pathways, that is, the one-bromine-atom abstraction (**Br-Abs**), the one-CBr_3-group-abstraction (**CBr_3-Abs**), and the insertion reaction (**Br-InS**). All were calculated at the B3LYP/6-311G(d) level of theory. The heavy arrows indicate the main components of the transition vector. Hydrogen atoms have been omitted for clarity.

[Eqs. (3a) and (3b); X and CX_3 abstraction], focusing on the transition states as well as the radical products. Starting from the precursor complex (**Pcx-F**, **Pcx-Cl**, **Pcx-Br**, and **Pcx-I** in Figures 1, 2, 3, 4, respectively), the reaction of dialkylsilylene (**10**) with CX_4 can take place in two ways: The abstraction of a halogen atom X from CX_4 to produce {silylene}–X$^{\bullet}$ and $CX_3^{\bullet}$ products (denoted **X-Abs**) and the radical transfer of $CX_3^{\bullet}$ to {silylene} leading to the formation of {silylene}–$CX_3^{\bullet}$ and X$^{\bullet}$ products (denoted **CX_3-Abs**), where {silylene} represents dialkylsilylene (**10**). That is to say, such single-electron-transfer radical mechanisms may proceed as follows: Reactants→precursor complex→transition state→radical products. The results for the transition states of the CX_4 radical reaction might perhaps be some of the most interesting of this study as very little is currently known about them.

The precursor complexes (**Pcx-F**, **Pcx-Cl**, **Pcx-Br**, and **Pcx-I**) all display similar {silylene}···(CX_4) bonding characteristics and the monomer geometries are essentially unperturbed. It was found that the distances between the carbon atom and the migrating halogen in the CX_4 moiety for the precursor complexes studied herein are somewhat elongated, that is, 1.331 (F), 1.796 (Cl), 2.011 (Br), and 2.462 Å (I) compared with 1.327 (F), 1.792 (Cl), 1.965 (Br), and 2.206 Å (I) for isolated CX_4. Moreover, the DFT results shown in Figures 1, 2, 3, and 4 reveal that the calculated bond distances for the Si···C contacts decrease from 4.775 (CF_4) to 3.650 (CCl_4) to 3.233 (CBr_4) to 2.740 Å (CI_4). Also, our B3LYP calculations indicate that the energies of these precursor complexes are all lower than those of the corresponding reactants by 0.71–7.9 kcal mol^{-1}. Nevertheless, as reported in Table 1, the Gibbs free energies demonstrate that the stabilization energies of all these precursor complexes are greater than those of the corresponding reactants. This strongly suggests that these precursor complexes should not exist at room temperature. We thus will not consider these precursor complexes further in this work.

Regarding the one-halogen-atom abstraction (X abstraction) mechanism, we have located the transition state for

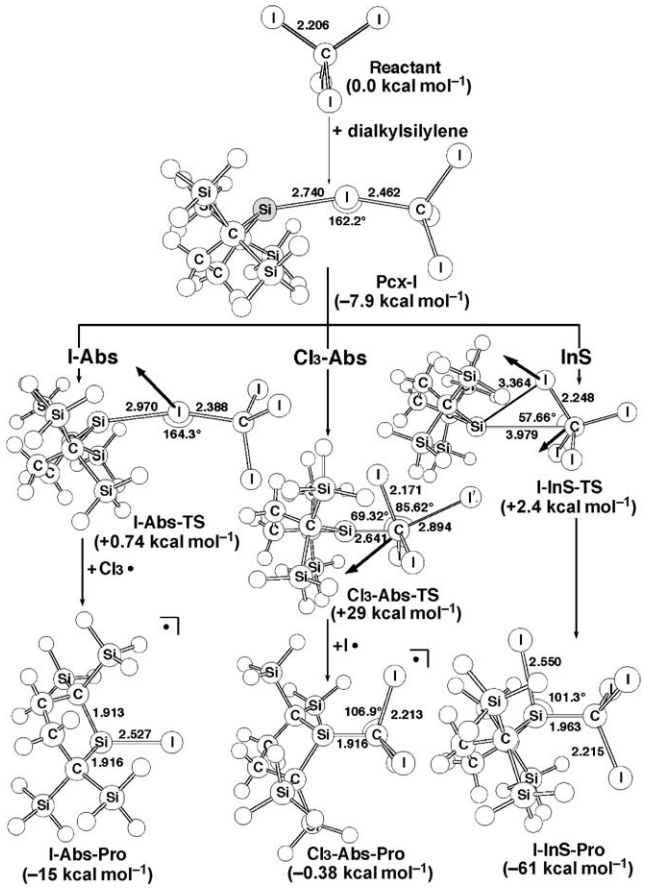

Figure 4. The optimized geometries (in Å and °) for the reactants, precursor complexes (**Pcx**), transition states (**TS**), and products (**Pro**) in the reaction of a stable dialkylsilylene with CI_4 through three reaction pathways, that is, the one-iodine-atom abstraction (**I-Abs**), the one-CI_3-group-abstraction (**CI_3-Abs**), and the insertion reaction (**I-InS**). All were calculated at the B3LYP/6-311G(d) level of theory. The heavy arrows indicate the main components of the transition vector. Hydrogen atoms have been omitted for clarity.

Table 1. Energies [kcal mol^{-1}] of stationary points relative to the reactants CX_4+stable silylene (X=F, Cl, Br, and I) at $T=0$ and 298.15 K (in square brackets).[a,b]

	CF_4	CCl_4	CBr_4	CI_4
$\Delta E_{st}=(E_{triplet}-E_{singlet})$	322.3	122.8	83.91	47.77
reactants: CX_4+{silylene}	0.0	0.0	0.0	0.0
precursor complex	−1.083 [5.587]	−0.7103 [6.512]	−2.277 [7.631]	−7.900 [2.962]
		X abstraction		
transition states	+35.74 [+47.30]	+3.417 [+14.71]	−2.111 [+11.57]	−7.156 [+3.870]
{silylene}−X•+CX_3• (radical products)	+10.92 [+10.35]	−12.45 [−13.00]	−14.24 [−15.18]	−15.34 [−16.05]
		CX_3 abstraction		
transition states	+79.66 [+92.02]	+47.17 [+60.17]	+40.36 [+53.71]	+29.17 [+42.81]
{silylene}−CX_3•+X• (radical products)	+76.22 [+80.40]	+23.54 [+28.23]	+12.30 [+17.19]	−0.3791 [+4.502]
		insertion		
transition states	+45.57 [+57.93]	+13.11 [+25.38]	+8.091 [+21.20]	+2.370 [+14.99]
insertion products	−69.27 [−56.06]	−72.54 [−58.01]	−68.33 [−53.09]	−60.53 [−44.91]

[a] Calculated at the B3LYP/6-311G(d) level of theory, see text. [b] See Figures 1–4 for structures.

each CX_4 (**F-Abs-TS**, **Cl-Abs-TS**, **Br-Abs-TS**, and **I-Abs-TS**) at the B3LYP level of theory. The structures and the main geometrical parameters of the four transition states are shown in Figures 1, 2, 3, and 4, respectively, along with the imaginary frequency eigenvectors. One can see that the main components of the transition vector correspond to the motion of the halogen atom (X) between the silicon and the carbon atom, whose eigenvalues give imaginary frequencies of 165*i* (**F-Abs-TS**), 151*i* (**Cl-Abs-TS**), 148*i* (**Br-Abs-TS**), and 126*i* cm^{-1} (**I-Abs-TS**). The transition states involve the approach of {silylene} along the X–C axis of the CX_4 molecule. The three atoms (Si, X, and C) involved in the bond-breaking and -forming processes are not co-linear along the X–C axis, as shown in Figures 1–4. The silicon atom of the {silylene} makes an angle, with respect to the X–C bond, of 155, 155, 158, and 164° for CF_4, CCl_4, CBr_4, and CI_4, respectively. Interestingly, the approach of the {silylene} along the X–C axis is more bent in the CF_4 and CCl_4 cases than in the CBr_4 and CI_4 cases. The breaking X–C bond length is generally increased and the forming Si–X bond length becomes smaller. For the reactions of {silylene} with CF_4, CCl_4, CBr_4, and CI_4, the breaking X–C bond lengths are 2.109 (F), 2.040 (Cl), 2.146 (Br), and 2.388 Å (I), respectively, whereas the forming Si–X bond lengths are 0.083 (F), 0.379 (Cl), 0.412 (Br), and 0.443 Å (I) longer than those in the {silylene}–X• product. This suggests that delocalization of the unpaired electron takes place later along the reaction coordinate. Thus, the Si–X and X–C bond lengths in the transition-state structure are more reactant-like for X=Br and I, in accordance with the large exothermicity of the abstraction process. As demonstrated below, this is consistent with the Hammond postulate[14] which associates an earlier transition state with a smaller barrier and a more exothermic reaction.

Moreover, the optimized geometries of the {silylene}–X• (**F-Abs-Pro**, **Cl-Abs-Pro**, **Br-Abs-Pro**, and **I-Abs-Pro**) radicals are also shown in Figures 1, 2, 3, and 4, respectively. Basically, these radicals adopt a SiL_3 pyramidal geometry. The B3LYP calculations show that in these radicals the Si–X bond distance is always longer than that in the corresponding CX_4 molecule (by about 0.320 Å). In addition, the flap angle at the carbon atom of the CX_3 radical (which is not shown in Figures 1–4) decreases uniformly as halogen X is changed from F (17.7) to Cl (10.2) to Br (9.35) and then to I (6.02°). That is to say, the geometry of the CX_3 radical becomes strongly pyramidal as halogen X becomes more electronegative.[15] In other words, pyramidalization at the CX_3 moiety decreases rapidly from F to I.

On the other hand, on considering the **CX_3-Abs** mechanism, a search for the transition state showed that the energy profile for this reaction exhibits a maximum. The transition states located for the CX_3 (X=F, Cl, Br, and I)

abstractions are presented in Figures 1, 2, 3, and 4, respectively. Each transition-state structure is characterized by one imaginary frequency: 580*i*, 483*i*, 484*i*, and 561*i* cm^{-1} for **CF_3-Abs-TS**, **CCl_3-Abs-TS**, **CBr_3-Abs-TS**, and **CI_3-Abs-TS**, respectively. The normal coordinate corresponding to the imaginary frequency is primarily the motion of the halogen atom ($X^{\bullet}$) separating from the carbon atom of CX_3. Therefore, the reaction coordinate is fundamentally an asymmetric stretch of the conventional transition state. Further, as was the case for the halogen-atom abstraction transition state (**X-Abs-TS**), the departing halogen atom $X^{\bullet}$ does not move along the Si–C axis. In addition, the transition-state structures reveal that the newly formed Si–C bond lengths are 2.279 (**CF_3-Abs-TS**), 2.446 (**CCl_3-Abs-TS**), 2.512 (**CBr_3-Abs-TS**), and 2.641 Å (**CI_3-Abs-TS**), compared with values in the radical product of 1.956 (**CF_3-Abs-Pro**), 1.951 (**CCl_3-Abs-Pro**), 1.937 (**CBr_3-Abs-Pro**), and 1.916 Å (**CI_3-Abs-Pro**), respectively. The C–F and C–Cl bond lengths are shorter (i.e., 2.279 Å in **CF_3-Abs-TS** and 2.446 Å in **CCl_3-Abs-TS**) and closer to those in the radical products (1.956 Å in **CF_3-Abs-Pro** and 1.951 Å in **CCl_3-Abs-Pro**). Taken together these features indicate that the transition-state structures for CF_4 and CCl_4 take on more product-like character than those of CBr_4 and CI_4. This is consistent with the greater exothermicity of the {silylene}+CX_4 reactions for X=Br and I (see below).

Furthermore, the equilibrium geometries for the {silylene}–$CX_3^{\bullet}$ (**CF_3-Abs-Pro**, **CCl_3-Abs-Pro**, **CBr_3-Abs-Pro**, and **CI_3-Abs-Pro**) radical products are presented in Figures 1, 2, 3, and 4, respectively. As in the case of the **X-Abs-Pro** species, all of these radical products adopt a SiL_3 pyramidal geometry. The DFT calculations suggest that the *trans* Si–C bond lengths decrease in the order **CF_3-Abs-Pro** (1.956) > **CCl_3-Abs-Pro** (1.951) > **CBr_3-Abs-Pro** (1.937) > **CI_3-Abs-Pro** (1.916 Å). Again, this result confirms the conventional finding that substitution of a more electronegative ligand (such as CF_3 and CCl_3) will strengthen the Si–C bond.

In the one-halogen-atom abstraction (X abstraction) approach, examination of the energy values collected in Table 1 shows that at the B3LYP/6-311G(d) level of theory Br and I abstractions are favored. Schematic diagrams for the {silylene}+CX_4 (X=F, Cl, Br, and I) reaction by X abstraction are displayed in Figures 1, 2, 3, and 4, respectively. The calculations performed in this work predict that the energies of **F-Abs-TS**, **Cl-Abs-TS**, and **Br-Abs-TS** are above those of the reactants by 35.740, 3.417, and −2.111 kcal mol^{-1} and the activation energies for the overall reaction are 36.80, 4.13, and 0.166 kcal mol^{-1}, respectively. In contrast, the DFT calculations suggest that the energies of **Br-Abs-TS** and **I-Abs-TS** are lower than those of the reactants, so that no net barrier to reaction exists. In addition, the activation energies from the corresponding precursor complex for Br and I abstraction are 0.166 and 0.744 kcal mol^{-1}, respectively. This is consistent with the observations shown earlier, in which, for the case of CBr_4 and CI_4, the saddle point lies much closer to the reactants than to the products. Consideration of the Gibbs free energies presented in Table 1 shows that the energies of all the transition states are greater than those of the corresponding reactants. Also, the trends in both the activation barriers and the reaction enthalpies are the same, even at room temperature. Moreover, for a given dialkylsilylene, the following general comments can be made. 1) The most dramatic change in the position of radical product along the reaction path occurs with **F-Abs-Pro**. The energy of **F-Abs-Pro** is apparently higher than the energy of the corresponding reactants by 10.9 kcal mol^{-1}, whereas the energies of the other radicals are lower than those of the reactants. This strongly suggests that fluorine atom abstraction should not occur in the reaction of dialkylsilylene (**10**) with a fluoroalkane. 2) The overall X-abstraction reaction is exothermic in each CX_4 case (with the exception of CF_4, as discussed above) and the enthalpy becomes more negative moving from fluorine to iodine. 3) The overall barrier heights are found to decrease in the order $CF_4 > CCl_4 > CBr_4 > CI_4$. This reflects the greater ease of abstracting a halogen from CBr_4 or CI_4 than from CF_4 or CCl_4. That is to say, the heavier the halogen atom (X), the more facile it is to abstract from CX_4.

The energetics of the CX_3-abstraction reactions are also summarized in Table 1 and Figures 1–4. The energies of the CX_3-abstraction reaction are calculated to be 79.7 (**CF_3-Abs-TS**), 47.2 (**CCl_3-Abs-TS**), 40.4 (**CBr_3-Abs-TS**), and 29.2 kcal mol^{-1} (**CI_3-Abs-TS**), respectively, all higher than their reactants. Note that the forward barrier to abstracting a CX_3 group from CX_4 for X=Cl, Br and I is about half that of the CF_4 case. Accordingly, our theoretical results reaffirm the Hammond postulate discussed earlier and predict that the process of abstracting a CBr_3 or CI_3 group should be easier than that of abstracting a CF_3 or CCl_3 group. From another point of view, this strongly implies that the leaving group tendency increases in the order F < Cl < Br < I. Moreover, this result reinforces the trend that the bonding energy of C–X decreases in the order C–F (116) > C–Cl (78.2) > C–Br (68) > C–I (51 kcal mol^{-1}).[15]

Finally, comparison of the CX_4-abstraction pathways for X=F, Cl, Br, and I reveals some interesting similarities and differences. The energetics of the X- and CX_3-abstraction reactions are summarized in Figure 5. As for the similarities, two similar abstraction pathways (X and CX_3 abstraction) exist for each CX_4 case. In particular, the enthalpies computed at the B3LYP/6-311G(d) level of theory are 10.9 kcal mol^{-1} for **F-Abs-Pro** in the fluorine abstraction process (X abstraction) and 76.2 kcal mol^{-1} for **CF_3-Abs-Pro** in the CF_3 abstraction process (CX_3 abstraction). That is, our theoretical findings demonstrate that the abstraction reactions of dialkylsilylene (**10**) with fluoroalkanes should not occur. Although the similarities between the two pathways are remarkable, the differences between them are more significant. The most notable differences are the barrier heights and the reaction enthalpies of the abstraction reactions. The activation barrier for the one-halogen-atom abstraction (X abstraction) mechanism is always less than that for the one-CX_3-group abstraction (CX_3-abstraction) mechanism. The reason for this is presumably the smaller repulsion between

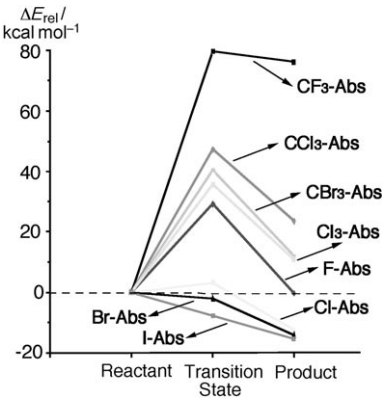

Figure 5. Reaction energy profile for the radical pathways (X and CX_3 abstraction) of the {silylene}+CX_4 reaction. All the energies were calculated at the B3LYP/6-311G(d) level of theory (see Table 1).

the halogen atom (X) and the substituents of the dialkylsilylene (**10**). That is, the site of the dialkylsilylene moiety is congested. As a result, it is easier for CX_4 to approach the silicon atom of dialkylsilylene (**10**) by X abstraction than by CX_3 abstraction. Moreover, our theoretical investigations suggest that the energies of the CX_3-abstraction products are higher than those of their corresponding reactants, except for the CI_3-abstraction system. This strongly indicates that this type of reaction is energetically very unfavorable, and that, if it did occur, the reactions would be endothermic as opposed to exothermic for the corresponding one-halogen-atom abstractions.

In brief, the calculations suggest the following about the radical mechanism for the {silylene}+CX_4 reaction. 1) Carbon–halogen activation may proceed by a two-step abstraction–recombination path (formation of two radicals collapsing in a subsequent step to give the final product). 2) The reaction rates for {silylene}+CF_4 and CCl_4 by the X- and CX_3-abstraction routes are expected to be significantly lower than those for CBr_4 and CI_4. 3) The one-halogen-atom abstraction pathway is much more favorable than the one-CX_3-group abstraction route from kinetic as well as theoretical considerations. This is consistent with the experimental observation that only the one-halogen-atom abstraction products are formed.[1c]

Mechanism for the insertion reactions: Let us next consider the insertion reactions of {silylene} into X–CX_3 [Eq. (3c)]. The corresponding reaction energy profiles for CX_4 (X=F, Cl, Br, and I) are again given in Figures 1, 2, 3, and 4, respectively. Some interesting conclusions can be drawn from these figures and the data given in Table 1.

The optimized transition-state structures for **F-InS-TS**, **Cl-InS-TS**, **Br-InS-TS**, and **I-InS-TS** along with the calculated transition vectors for the four insertion reactions are shown in Figures 1, 2, 3, and 4, respectively. The arrows in the figures illustrate the direction in which the atoms move in the normal coordinate corresponding to the imaginary frequency. Examination of the single imaginary frequency for each transition state ($488i\ cm^{-1}$ for **F-InS-TS**, $248i\ cm^{-1}$ for **Cl-InS-TS**, $135i\ cm^{-1}$ for **Br-InS-TS**, and $130i\ cm^{-1}$ for **I-InS-TS**) provides excellent confirmation of the insertion process. The vibrational motion for the addition of CX_4 to {silylene} involves bond formation between silicon and carbon in concert with the breaking of the C–X bond and halogen transfer to the adjacent silicon atom. Indeed, the main similarity in the transition states is the three-center pattern involving the silicon, carbon, and halogen atoms. Note that such characteristic three-center transition states are quite analogous to the mechanisms observed in the oxidative addition of C–H bonds to carbene-like ML_n fragments.[16]

Furthermore, the B3LYP/6-311G(d) results show that in **F-InS-TS** and **Cl-InS-TS** the Si–C and Si–X (X=F and Cl) distances and the C-Si-X angle are similar in magnitude to those in the corresponding radical product (see Figures 1 and 2, respectively). On the other hand, in **Br-InS-TS** and **I-InS-TS** the Si–C and Si–X (X=Br and I) distances are longer than those of the corresponding products. These features indicate that the C–Br and C–I insertion reactions reach the transition state relatively early, whereas in the C–F and C–Cl insertion reactions the transition state is reached relatively late. In other words, the heavier the tetrahalomethane system, the more reactant-like the transition-state structure. Accordingly, as in the abstraction processes discussed previously, one may anticipate a smaller barrier to CBr_4 and CI_4 insertion (see above).

The calculated reaction profiles for {silylene} insertion into CX_4 (X=F, Cl, Br, and I) are collected in Figure 6. Indeed, on examination of Figure 6 and Table 1, it is clear that, from a kinetic viewpoint, the insertion reactions of CX_4 for X=Cl, Br, and I are much more favorable than that of the CF_4 molecule. For example, the DFT results suggest that the barrier heights for the insertions decrease in the order **F-InS-TS** (45.6) > **Cl-InS-TS** (13.1) > **Br-InS-TS** (8.09) > **I-InS-TS** (2.37 kcal mol^{-1}). Note that the activation barrier for the iodine insertion is smaller than those for the

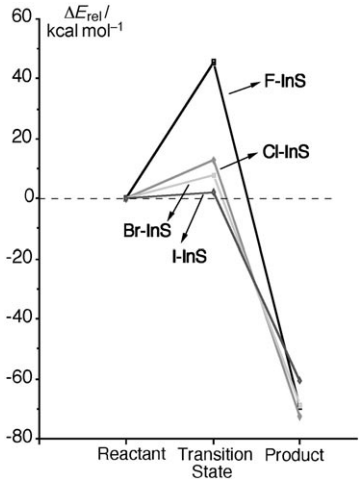

Figure 6. Reaction energy profile for the insertion pathways (**InS**) of the {silylene}+CX_4 reaction. All the energies were calculated at the B3LYP/6-311G(d) level of theory (see Table 1).

other halogen analogues. Similarly, as one can see in Figures 1, 2, 3, and 4 as well as Table 1, it is clear that all the insertion reactions are thermodynamically exothermic. The order of exothermicity follows the similar trend as that of the activation energy: **Cl-InS-Pro** (-72.5) > **F-InS-Pro** (-69.3) > **Br-InS-Pro** (-68.3) > **I-InS-Pro** (-60.5 kcal mol^{-1}). It is therefore predicted that the heavier the halogen, the easier the insertion reaction of tetrahalomethanes. Moreover, the {silylene}+CX_4 (X = F, Cl, Br, and I) reactions occur in a concerted fashion as no other intermediates have been found in such a process at this level of calculation.

In short, two intriguing conclusions are worth noting. 1) The carbon–halogen insertion reaction into dialkylsilylene (**10**) is not only concerted (proceeding without formation of an intermediate), but also synchronous (with bond-forming and -breaking occurring simultaneously in transition states of lower energy). 2) As can be seen in Table 1, the barrier heights for the reaction of dialkylsilylene (**10**) with CX_4 should increase in the order: X abstraction < insertion < CX_3 abstraction. On the other hand, the reaction enthalpies for the same reactions decrease in the order CX_3 abstraction > X abstraction > insertion. That is to say, the one-halogen-atom abstraction (X abstraction) should be the fastest reaction from a kinetic viewpoint. In contrast, only the insertion reaction can produce a thermodynamically stable product.

Overview of the dialkylsilylene reactions with CX_4: From our survey of the mechanisms of the {silylene}+CX_4 reactions, we come to the following conclusions:

1) For the dialkylsilylene system studied herein, precursor complexes for the haloalkane reaction should not be observable at room temperature.
2) By considering both the calculated activation barriers and the reaction enthalpies, we conclude that for the reaction of dialkylsilylene with carbon tetrahalides, the order of reactivity is always I > Br > Cl ≫ F, no matter what kind of reaction is involved. This may be a reflection of the C–X bond strengths.
3) Of the three kinds of dialkylsilylene + haloalkane reactions (X and CX_3 abstraction and insertion), the X-abstraction mechanism is the most kinetically favorable, whereas the insertion mechanism is the most thermodynamically favorable. Indeed, the X-abstraction reaction is mostly observed in many related experiments.[1c]
4) The SET mechanism occurs by either X or CX_3 abstraction by the dialkylsilylene and recombination of the intermediates [see Eqs. (3a) and (3b)]. Regardless of which haloalkane is considered, one-halogen-atom abstraction (X abstraction) is highly favored compared with one-CX_3-group abstraction (CX_3 abstraction) from both kinetic and thermodynamic viewpoints.
5) Our theoretical findings based on the Gibbs free energy calculations suggest that the magnitudes of the X-abstraction (X = Cl, Br, and I) barriers are very small. This implies that radical reactions of stable dialkylsilylenes with haloalkanes should be facile processes at room temperature.
6) The insertion reactions between dialkylsilylene and haloalkanes can produce a thermodynamically stable product, although this reaction is not kinetically favored. This theoretical finding is in agreement with one available experimental observation.[1c]
7) Electronic as well as steric factors should play a dominant role in determining the chemical reactivity of stable dialkylsilylene species, kinetically as well as thermodynamically.

Origin of the barrier height and the reaction enthalpy for reaction of a stable dialkylsilylene: From our above theoretical analysis, all our computations can be rationalized on the basis of the configuration-mixing (CM) model developed by Pross and Shaik.[17,18] From this model, one may easily understand that the energy barriers governing the processes as well as the reaction enthalpies should depend on the singlet–triplet splitting ΔE_{st} ($=E_{triplet}-E_{singlet}$) in the stable dialkylsilylene (**10**) and the σ–σ* energy gap $\Delta E_{\sigma\sigma^*}$ ($=E_{\sigma^*}-E_{\sigma}$) of the CX_4 molecule. That is, the smaller the value of $\Delta E_{st}+\Delta E_{\sigma\sigma^*}$, the lower the barrier height and the greater the exothermicity.[17,18]

Bearing the above conclusions in mind, the origin of the trends detailed below can be explained.

1) Why does the ease of halogen abstraction or insertion from CX_4 increase in the order C–F ≪ C–Cl < C–Br < C–I? According to the CM model stated above, it is readily seen that the magnitude of $\Delta E_{\sigma\sigma^*}$ for a carbon tetrahalide CX_4 should play a key role in determining the reactivity order for the abstractions or insertions of a stable dialkylsilylene. That is, a smaller $\Delta E_{\sigma\sigma^*}$ for the CX_4 species results in a lower barrier height and a greater exothermicity. This would lead to fast abstraction or insertion between the stable dialkylsilylene and the CX_4 species. A qualitative diagram showing the relative σ and σ* energy levels for the C–X bonds is given in Figure 7.[19] As one can see in this diagram, the energies of the σ orbitals increase from fluorine to

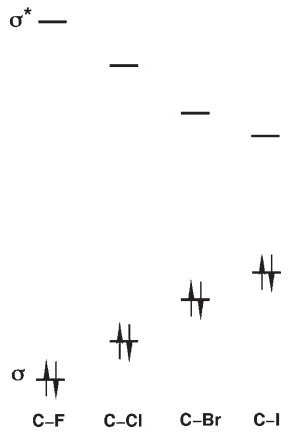

Figure 7. Schematic representation of the relative energy levels of the σ and σ* orbitals of the C–F, C–Cl, C–Br, and C–I bonds (see ref. [19]).

iodine. Namely, $\sigma(C{-}F) < \sigma(C{-}Cl) < \sigma(C{-}Br) < \sigma(C{-}I)$. On the other hand, the energies of the σ* orbitals decrease from fluorine to iodine. Namely, $\sigma^*(C{-}F) > \sigma^*(C{-}Cl) > \sigma^*(C{-}Br) > \sigma^*(C{-}I)$. In other words, the $\sigma(C{-}X) \rightarrow \sigma^*(C{-}X)$ triplet excitation energies for CX_4 decrease along the series fluorine to iodine. Our B3LYP calculations indicate a decrease in $\Delta E_{\sigma\sigma^*}$ in the order CF_4 (322) > CCl_4 (123) > CBr_4 (83.9) > CI_4 (47.8 kcal mol^{-1}). In consequence, our DFT results are in perfect agreement with the above prediction. Indeed, it has been experimentally reported that the bonding energies for C–F, C–Cl, C–Br, and C–I are 116, 78.2, 68, and 51 kcal mol^{-1}, respectively,[20] in good agreement with the above prediction.

From the reverse point of view, this means that the order of radical reactivity should increase in the order $F^{\bullet} < Cl^{\bullet} < Br^{\bullet} < I^{\bullet}$ and $CF_3^{\bullet} < CCl_3^{\bullet} < CBr_3^{\bullet} < CI_3^{\bullet}$. From Table 1 it is apparent that the above predictions are in good agreement with the trend in activation energy as well as reaction enthalpy (ΔE_a, ΔH) for halogen abstraction [Eq. (3a)], CX_3 abstraction [Eq. (3b)], and C–X insertion [Eq. (3c)]. Accordingly, the investigations presented in this work provide strong evidence that the singlet–triplet gap ($\Delta E_{\sigma\sigma^*}$) plays a decisive role in determining the reactivity of haloalkanes.

2) Given identical single-electron-transfer reaction conditions, why is the one-halogen-atom abstraction favored over the one-CX_3-group abstraction? Again, the driving force for this can be easily understood from the bonding energies. That is, the reactivity order for X and CX_3 abstractions may be traced to the relative strengths of the Si–X (X = halogen) and Si–C bonds. The thermodynamic reactions in Equation (4) can be used to evaluate the bond energies. As a result, the energy difference ΔE(BDE) between the Si–X and Si–C bonds can be determined from Equation (5).

$$\{\text{silylene}\}{-}X \rightarrow \{\text{silylene}\}^{\bullet} + X^{\bullet} \qquad \Delta E_1 \tag{4a}$$

$$\{\text{silylene}\}{-}CX_3 \rightarrow \{\text{silylene}\}^{\bullet} + CX_3^{\bullet} \qquad \Delta E_2 \tag{4b}$$

$$\Delta E(\text{BDE}) = \Delta E_1 - \Delta E_2 \tag{5}$$

Indeed, the values determined from Equation (5) can be obtained from the differences in the energies of the X- and CX_3-abstraction reactions (Table 1), which were calculated to be 70.1, 41.2, 32.4, and 20.6 kcal mol^{-1} for CF_4, CCl_4, CBr_4, and CI_4, respectively. These values thus strongly support the notion that the bonding energy of Si–X is much stronger than that of Si–CX_3 and therefore that {silylene}–X is more stable than {silylene}–CX_3. Consequently, our theoretical findings demonstrate that the one-halogen-atom abstraction path is favored over the one-CX_3-group abstraction route.

Conclusion

In conclusion, great success has recently been achieved in the synthesis and characterization of stable dialkylsilylene and haloalkane systems, although even just a few years ago such systems would have been considered inaccessible. However, the mechanisms of the synthetic reactions had not been established either by experimental physicochemical methods or by theoretical calculations. We have now presented the first theoretical study of the mechanisms of the reactions of a stable dialkylsilylene with carbon tetrahalides. With the above analysis in mind, one can see that, for a given stable dialkylsilylene, the lower the electronegativity of the halogen atom in the haloalkane, the smaller its $\Delta E_{\sigma\sigma^*}$, and, in turn, the more rapid its one-halogen-atom abstraction from a saturated C–X bond. This kind of abstraction from a haloalkane can lead to a new silyl radical, which can either yield a new dihalosilane molecule or the observed coupling products by radical recombination.[1c] In addition, our computational results show that insertion reactions can lead to a thermodynamically stable product. Although in principle these two reactions may compete with other, in practice, it is likely that the one-halogen abstraction path is favored for kinetic reasons. These theoretical predictions are consistent with the available experimental observations.[1c]

Furthermore, as our analysis demonstrates, the CM approach adds additional facets and insights into this relatively poorly understood area of mechanistic study. Although the relative reactivity of the stable dialkylsilylene is determined by the entire potential-energy surface, the concepts of the CM model, focusing on the singlet–triplet splitting in the reactants, allows one to assess quickly the relative reactivity of a variety of stable dialkylsilylenes without specific knowledge of the actual energies of the interactions involved. In spite of its simplicity, our approach can provide chemists with important insights into the factors controlling the activation energies of halogen-atom transfer reactions.

We encourage experimental chemists to carry out further experiments to confirm our predictions.

Acknowledgements

The authors are grateful to the National Center for High-Performance Computing of Taiwan for generous amounts of computing time. They also thank the National Science Council of Taiwan for the financial support.

[1] For recent reviews, see: a) P. P. Gaspar, R. West in *The chemistry of Organic Silicon Compounds*, 2nd ed. (Eds.: Z. Rappoport, Y. Apeloig), Wiley, New York, **1999**, Part 3, p. 2463; b) M. Haaf, T. A. Schmedake, R. West, *Acc. Chem. Res.* **2000**, *33*, 704; c) N. J. Hill, R. West, *J. Organomet. Chem.* **2004**, *689*, 4165; d) M. Weidenbruch, *Eur. J. Inorg. Chem.* **1999**, 373; e) B. Gehrhus, M. F. Lappert, *J. Organomet. Chem.* **2001**, *617*, 209; f) B. Gehrhus, P. B. Hitchcock, R. Pongtavornpinyo, L. Zhang, *Dalton Trans.* **2006**, *15*, 1847.

[2] The electronic nature of heteroatom-substituted silylenes remains a controversial topic: a) D. A. Dixon, K. B. Dobbs, A. J. Arduengo III, G. Bertrand, *J. Am. Chem. Soc.* **1991**, *113*, 8782; b) R. Dagani, *Chem. Eng. News* **1991**, *69*, 19; c) M. Regitz, *Angew. Chem.* **1991**, *103*, 691; *Angew. Chem. Int. Ed. Engl.* **1991**, *30*, 674; d) R. Dagani, *Chem. Eng. News* **1994**, *72*, 20; e) C. Heinemnn, T. Muller, Y. Apeloig, H. Schwartz, *J. Am. Chem. Soc.* **1996**, *118*, 2023; f) C. Boehme, G. Frenking, *J. Am. Chem. Soc.* **1996**, *118*, 2039; g) T. Veszpremi, L.

Nyulaszi, B. Hajgato, J. Heinicke, *THEOCHEM* **1998**, *431*, 1; h) R. West, J. J. Buffy, M. Haaf, T. Muller, B. Gehrhus, M. F. Lappert, Y. Apeloig, *J. Am. Chem. Soc.* **1998**, *120*, 1639.

[3] For instance, see: a) D. Moser, A. Naka, I. A. Guzei, T. Muller, R. West, *J. Am. Chem. Soc.* **2005**, *127*, 2691; b) A. G. Avent, B. Gehrhus, P. B. Hitchcock, M. F. Lappert, H. Maciejewski, *J. Organomet. Chem.* **2003**, *686*, 321; c) R. West, T. A. Schmedake, M. Haaf, J. Becker, T. Mueller, *Chem. Lett.* **2001**, 68; d) A. Naka, N. J. Hill, R. West, *Organometallics* **2004**, *23*, 6330.

[4] For **1**, see: a) M. Denk, R. Lennon, R. Hayashi, R. West, A. Haaland, H. Belyakov, P. Verne, M. Wagner, N. Metzler, *J. Am. Chem. Soc.* **1994**, *116*, 2691; b) M. Haaf, A. Schmiedel, T. A. Schmedake, D. R. Powell, A. J. Millevolte, M. Denk, R. West, *J. Am. Chem. Soc.* **1998**, *120*, 12714.

[5] For **2**, see: a) R. West, M. Denk, *Pure Appl. Chem.* **1996**, *68*, 785; b) M. Haaf, T. A. Schmedake, B. J. Paradise, R. West, *Can. J. Chem.* **2000**, *78*, 1526.

[6] For **3**, see: a) B. Gehrhus, M. F. Lappert, J. Heinicke, R. Boose, D. Blaser, *J. Chem. Soc., Chem. Commun.* **1995**, 1931; b) B. Gehrhus, P. B. Hitchcock, M. F. Lappert, J. Heinicke, R. Boose, D. Blaser, *J. Organomet. Chem.* **1996**, *521*, 211.

[7] For **4**, see: J. Heinicke, A. Oprea, M. K. Kindermann, T. Karpati, L. Nyulaszi, T. Veszpremi, *Chem. Eur. J.* **1998**, *4*, 541.

[8] For **5**, see: a) M. Kira, S. Ishida, T. Iwamoto, C. Kabuto, *J. Am. Chem. Soc.* **1999**, *121*, 9722; b) S. Ishida, T. Iwamoto, C. Kabuto, M. Kira, *Chem. Lett.* **2001**, 1102.

[9] M.-D. Su, S.-Y. Chu, *J. Am. Chem. Soc.* **1999**, *121*, 1045.

[10] For simplicity, in this study we substitute the SiH_3 group for the $SiMe_3$ group.

[11] a) A. D. Becke, *Phys. Rev. A*, **1988**, 38, 3098; b) A. D. Becke, *J. Chem. Phys.* **1993**, *98*, 5648; c) C. Lee, W. Yang, R. G. Parr, *Phys. Rev. B* **1988**, *37*, 785; d) B. Miehlich, A. Savin, H. Stoll, H. Preuss, *Chem. Phys. Lett.* **1989**, *157*, 200.

[12] T. H. Dunning, Jr., P. J. Hay in *Modern Theoretical Chemistry* (Ed.: H. F.Schaefer III), Plenum Press, New York, **1976**, pp. 1–28.

[13] Gaussian 03, Revision C.02, M. J. Frisch, G. W. Trucks, H. B. Schlegel, G. E. Scuseria, M. A. Robb, J. R. Cheeseman, J. A. Montgomery, Jr., T. Vreven, K. N. Kudin, J. C. Burant, J. M. Millam, S. S. Iyengar, J. Tomasi, V. Barone, B. Mennucci, M. Cossi, G. Scalmani, N. Rega, G. A. Petersson, H. Nakatsuji, M. Hada, M. Ehara, K. Toyota, R. Fukuda, J. Hasegawa, M. Ishida, T. Nakajima, Y. Honda, O. Kitao, H. Nakai, M. Klene, X. Li, J. E. Knox, H. P. Hratchian, J. B. Cross, V. Bakken, C. Adamo, J. Jaramillo, R. Gomperts, R. E. Stratmann, O. Yazyev, A. J. Austin, R. Cammi, C. Pomelli, J. W. Ochterski, P. Y. Ayala, K. Morokuma, G. A. Voth, P. Salvador, J. J. Dannenberg, V. G. Zakrzewski, S. Dapprich, A. D. Daniels, M. C. Strain, O. Farkas, D. K. Malick, A. D. Rabuck, K. Raghavachari, J. B. Foresman, J. V. Ortiz, Q. Cui, A. G. Baboul, S. Clifford, J. Cioslowski, B. B. Stefanov, G. Liu, A. Liashenko, P. Piskorz, I. Komaromi, R. L. Martin, D. J. Fox, T. Keith, M. A. Al-Laham, C. Y. Peng, A. Nanayakkara, M. Challacombe, P. M. W. Gill, B. Johnson, W. Chen, M. W. Wong, C. Gonzalez, J. A. Pople, Gaussian, Inc., Wallingford CT, **2004**.

[14] G. S. Hammond, *J. Am. Chem. Soc.* **1954**, *76*, 334.

[15] The C–X (X = F, Cl, Br, and I) bond energy is 116, 78.2, 68, and 51 $kcal\,mol^{-1}$, respectively; see: J. E. Huheey, E. A. Keiter, R. L. Keiter, *Inorganic Chemistry*, 4th ed., Harper Collins College Publishers, New York, **1993**.

[16] For instance, see: M.-D. Su, S.-Y. Chu, *J. Am. Chem. Soc.* **1999**, *121*, 1045.

[17] For details, see: a) S. Shaik, H. B. Schlegel, S. Wolfe in *Theoretical Aspects of Physical Organic Chemistry*, Wiley, New York, **1992**; b) A. Pross in *Theoretical and Physical Principles of Organic Reactivity*, Wiley, New York, **1995**; c) S. Shaik, *Prog. Phys. Org. Chem.* **1985**, *15*, 197.

[18] a) For the first paper that originated the CM model, see: S. Shaik, *J. Am. Chem. Soc.* **1981**, *103*, 3692; b) for the most up-to-date review of the CM model, see: S. Shaik, A. Shurki, *Angew. Chem.* **1999**, *111*, 616; *Angew. Chem. Int. Ed.* **1999**, *38*, 586.

[19] A. Pross, *Theoretical and Physical Principles of Organic Reactivity*, Wiley, New York, **1995**, p. 51.

[20] J. E. Hueey, E. A. Keiter, R. L. Keiter, *Inorganic Chemistry*, 4th ed., Harper Collins College Publishers, New York, **1993**.

Received: December 4, 2006
Published online: May 31, 2007

